Electrorefraction in strained InGaAs/InP chopped quantum wells : significance of the interface layers

Electrorefraction in strained InGaAs/InP chopped quantum wells: Significance of the interface layers

B. H. P. Dorren, A. Yu. Silov, M. R. Leys, J. E. M. Haverkort,[a] and J. H. Wolter
COBRA Inter-University Research Institute, Eindhoven University of Technology, P.O. Box 513, 5600 MB Eindhoven, The Netherlands

(Received 3 February 1999; accepted for publication 22 November 1999)

We present a model for electrorefraction based on the quantum confined Stark effect (QCSE) in strained InGaAs/InP chopped quantum wells (CQWs) consisting of three 27 Å InGaAs wells separated by 15 Å InP barriers. The model fully takes into account the influence of the thin interface layers around each well. We experimentally verify the model on a InGaAs/InP CQW which combines a large 60 meV QCSE redshift at 11.7 V bias with waveguide transparency at 1.55 μm, which is two times larger than in a InGaAsP quaternary well. The calculated electroabsorption spectra of the CQWs are in good agreement with experiment. We finally applied the Kramers–Kronig transformations for calculating the switching voltage in a Mach–Zehnder switch employing CQWs in the phase shifting section. The model was found to be in good agreement with experiment for both polarizations. © *2000 American Institute of Physics.* [S0021-8979(00)08005-1]

I. INTRODUCTION

Mach–Zehnder interferometric switches and waveguide electrorefraction modulators require a low loss material with large and polarization independent electrorefraction at 1.55 μm. In principle, it is well known that the quantum confined Stark effect (QCSE) in InGaAs/InP[1,2] provides a large electroabsorption which also translates into electrorefraction through the Kramers–Kronig transformations. Since device operation requires the InGaAs/InP quantum wells to be transparant for waveguide propagation at 1.55 μm, a large detuning between the band gap and the operating wavelength is necessary. Such a large detuning unfortunately reduces electrorefraction at the operating wavelength considerably. A second device requirement is a polarization independent electrorefraction. It is virtually impossible to optimize a quantum well structure for these mutually conflicting device requirements without having an accurate design tool which is capable of calculating the electrorefraction starting from an arbitrary strained quantum well structure.

We will present a model that allows us to calculate the electroabsorption spectra taking into account the interface layers[3,4] around each individual InGaAs/InP well which were hitherto neglected. Our model also accounts for the complex nature of the valence band[5] in order to properly calculate the polarization dependence of the device. We will show that both these aspects are necessary for properly calculating the electroabsorption and refraction. In this article we apply and experimentally verify the model on strained InGaAs/InP chopped quantum well (CQW) structures that combine a very large QCSE redshift with waveguide transparancy at 1.55 μm. We show that these CQWs are suitable for application as a polarization independent, low loss waveguide electrorefraction modulator. It will finally be shown that the model is able to describe the measured electrorefraction with reasonable accuracy when the interface layers are properly taken into account.

II. MODEL

To predict the polarization dependence of the switches, it is important that we include all strained material including the interface layers between each quantum well and its cladding. The composition and the thickness of the interface layers in chemical beam epitaxy was studied by Rongen *et al.*[6] using x-ray diffraction and photoluminescence experiments in samples grown in the same machine. A smoothening time of 2 s and a substitution time of 1 s at the lower $In_{1-x}Ga_xAs$ interface leads to a 1 monolayer (ML) InAs interface layer. The upper interface consists of a 1 ML $In_{1-0.5x}Ga_{0.5x}As_{0.5}P_{0.5}$ interface. Furthermore, a small As gradient[7] in the InP above the InGaAs well was found to be present.

When we intend to grow a chopped quantum well consisting of three strongly coupled 27 Å wide InGaAs wells separated by 15 Å barriers, the resulting structure includes interface layers as shown in Fig. 1. This potential, which will be used in our model calculations, is somewhat simplified since we stoichiometrically averaged the upper interface and the thin InP barrier with the As gradient yielding a 15 Å $In_{0.95}Ga_{0.05}As_{0.2}P_{0.8}$ layer.

To calculate the electroabsorption we developed a model based on the 4×4 Luttinger–Kohn Hamiltonian. The model-solid theory[8] is used to account for the strain. The ternary band gaps were interpolated using bowing parameters according to Ref. 9. The remaining parameters were linearly interpolated from Ref. 10. Using the calculated dispersion relations and the optical matrix elements in dipole approximation we calculated the absorption spectra[11] including up to

[a]Author to whom correspondence should be addressed; electronic mail: haverkort@cobra.tue.nl

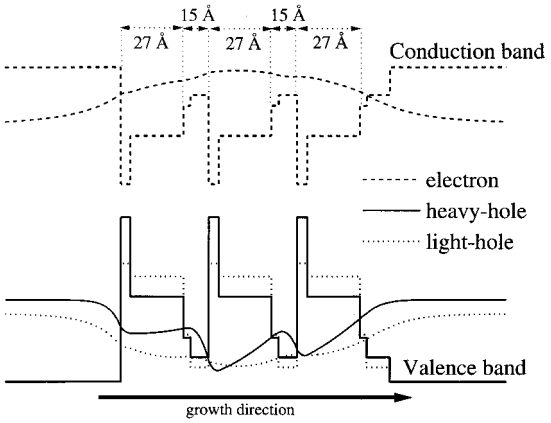

FIG. 1. An InGaAs/InP chopped quantum well structure including interfaces with the envelope wavefunctions for the holes and the electron.

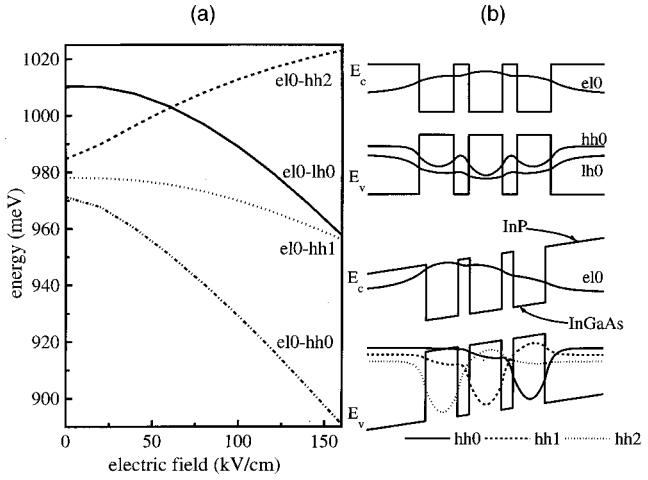

FIG. 2. (a) Calculated energy levels and energy level shifts for a chopped quantum well structure. (b) The CQW potential and the ground state envelope wave functions for electrons, heavy holes, and light holes without applied electric field (upper graph) and with an applied electric field of 75 kV/cm (lower graph).

six energy levels for each band. The absorption spectra were broadened with 8 meV hyperbolic cosine line shape function at low temperature. Electrorefraction spectra were subsequently calculated for both polarizations by taking a Kramers–Kronig transform[12] of the calculated near band gap electroabsorption spectra. The spectral integration range for the Kramers–Kronig integration was chosen as wide as possible, but this range was also carefully chosen to obey the sum rules.[13]

III. CHOPPED QUANTUM WELLS

In order to verify the model, we apply it to CQW structures which can be inserted into an efficient and low-loss polarization independent Mach–Zehnder switch operating at 1.55 μm. Waveguide transparancy in such a device constraints the band gap below 1400 nm[14] at room temperature. This in turn limits the InGaAs/InP quantum well thickness below 35 Å. Electrorefraction and electroabsorption modulators employing the QCSE, however, require much wider quantum wells for an appreciable QCSE since the QCSE redshift very rapidly increases with quantum well thickness.[2] It is well known that quaternary quantum wells allow us to increase the QCSE strongly while simultaneously preserving waveguide transparency at 1.55 μm.[2] At 100 kV/cm applied bias, a 35 Å InGaAs/InP quantum well shows a 1.5 meV QCSE redshift while a 110 Å $In_{0.6}Ga_{0.4}As_{0.85}P_{0.15}$ quantum well shows a 25 meV redshift. Coupled quantum wells offer even larger freedom in material design[15,16] and allow us to further increase the QCSE redshift. Three strongly coupled 27 Å wide InGaAs wells separated by 15 Å barriers, as shown in Fig. 2, combine the desired zero-bias band gap at 890 meV for waveguide transparency with an effective well width of 110 Å to assure a large QCSE. This CQW structure features a 45 meV QCSE redshift at 100 kV/cm applied bias. This is two times larger than in a single quaternary well of the same total well width and average composition.

In a CQW, the coupling between the individual wells is excellent for the light holes (lh) and the electrons (el) due to their small effective mass [see Fig. 2(b)]. For the electrons and lhs, the resulting QCSE redshift and envelope function deformation is similar as in a 110 Å wide quantum well with the average CQW composition. The hh potential approaches the limit of three uncoupled wells, since the hh coupling between the individual wells is much weaker. In the presence of an electric field, the ground-state hh_0 envelope wave function localizes in the right-side quantum well [see Fig. 2(b)], hh_1 localizes in the central well, and hh_2 localizes in the left-side quantum well. Since the energy levels within the two outermost quantum wells are strongly shifted due to the electric field, the el_0–hh_0 transition is 29 meV redshifted and the the el_0–hh_2 transition is 22 meV blueshifted at 75 kV/cm. Figure 2(a) shows the transition energy of these levels as a function of electric field.

IV. EXPERIMENT

To experimentally verify this large QCSE, we have grown three CQW samples in a *p-i-n* structure. Each sample consists of 20 CQWs and was grown on the (100) plane of a *n*-doped InP substrate. The intrinsic InGaAs/InP CQW layer was sandwiched between two 0.2 μm thick undoped InP cladding layers to assure low propagation loss and low carrier concentrations within the wells. To vary the splitting between the hh_0 and lh_0 levels, we have grown three samples with a tensile strain of 0.4%, 0.6%, and 0.8%, corresponding to $In_{1-x}Ga_xAs$ QWs with $x=0.525$, 0.555, and 0.585. The spacing between two neighboring CQWs was 155 Å to avoid mutual coupling. The background doping in the intrinsic region was $1-2\times10^{15}/cm^3$. The 1.2 μm *p*-type InP top layer of the sample was doped with $2-4\times10^{17}/cm^3$ Be and was capped with a 500 Å $1-2\times10^{19}/cm^3$ $In_{0.53}Ga_{0.47}As$ layer.

Room temperature photoluminescence measurements show peaks with a 45 meV FWHM at 876 meV (1414 nm), 888 meV (1395 nm), and 901 meV (1375 nm) for the samples with a Ga composition of 52.5%, 55.5%, and 58.5%, respectively. The calculated band gap for the sample with 52.5% Ga is 891 meV when the interface layers are included and 953 meV without the interfaces, showing that the interfaces shift the band gap by 60 meV. The residual difference

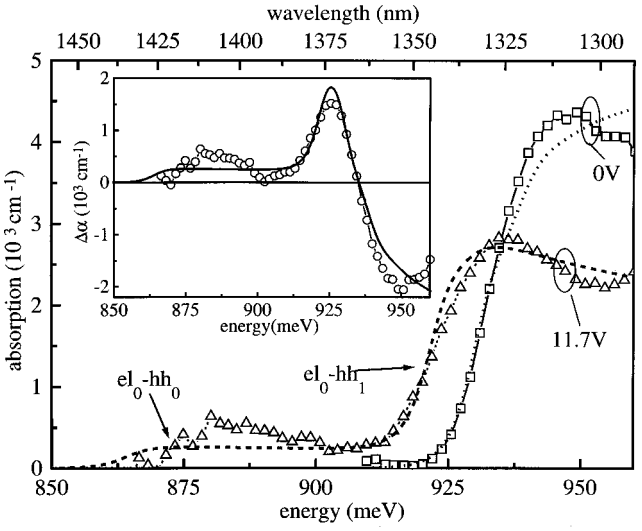

FIG. 3. Photocurrent measurements of the absorption spectra and calculated absorption spectra of the sample with a Ga concentration of 52.5%. Photocurrent measurements at 0 and 11.7 V are shown as squares and triangles, respectively. The calculations at 0 and 142 kV/cm are shown as dotted and dashed curves. The measured absorption heights were vertically scaled to the calculated ones. The inset shows the calculated (solid lines) and measured (circles) change of the electroabsorption spectra obtained.

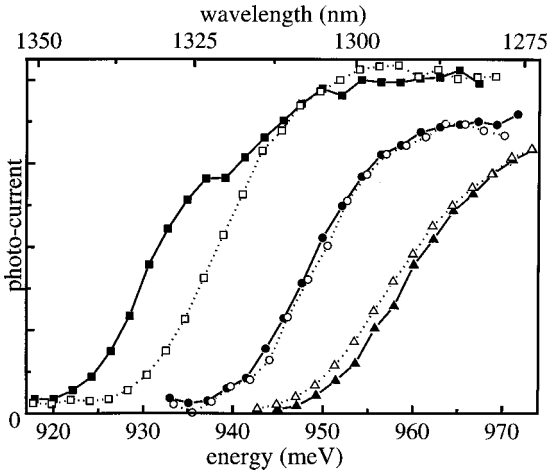

FIG. 4. TE (solid symbols) and TM (open symbols) cleaved side photocurrent measurements for the CQW samples with 52.5% (squares), 55.5% (circles), and 58.5% (triangles) gallium. The curves are drawn as a guide to the eye.

between the calculated and measured band gaps is due to the Stokes shift. The observed band gaps above 876 meV (below 1414 nm) confirm that waveguide transparency at 1550 nm is achievable with CQWs.

Photocurrent spectra on the $200\times200\ \mu$m mesa structures of the 52.5% Ga sample are shown for the unbiased and reverse biased sample at 50 K in Fig. 3 at an excitation density of 20 mW/cm^2. The curves are vertically scaled with respect to each other to correct for the different quantum efficiencies at different reverse bias. These measurements show an effective redshift of the lowest confined level in excess of 60 meV at 11.7 V reverse bias.

Calculated absorption spectra without bias (1.35 V built-in voltage) and 11.7 V applied bias over the 0.9 μm intrinsic region of the CQW are also shown in Fig. 3. The relative heights,[17] the energy level positions, and the broadening of the calculated spectra are in close agreement with the measurements confirming the validity of our model. The measured QCSE redshift is about 10 meV less than calculated, probably due to a lower build in electric field resulting from internal series resistances. The primary factor to establish this level of agreement between the model and the experimental data was to take into account the interface layers into our model. The inset of Fig. 3 shows the calculated and measured absorption difference spectra between 0 and 11.7 V applied bias for the sample with a Ga composition of 52.5%. Once more a very good agreement is observed between measurements and calculations.

TE and TM absorption spectra were subsequently measured by cleaved-side excitation photocurrent measurements. Figure 4 shows that the band gap is shifted 25 meV down with increasing Ga composition. The strong polarization dependence of the sample with 52.5% Ga vanishes as strain increases. Between a Ga concentration of 55.5% and 58.5% the light hole ground state crosses the lowest three almost degenerate hh levels and the band gap changes from hh to lh character.

The hh–lh splitting determines if the structure shows polarization independent behavior. The value of the hh–lh splitting is, however, strongly determined by the interfaces. As an example for the sample with $x=0.525$, the calculated hh–lh splitting increases with 11 meV when the interfaces are properly taken into account as compared to the situation where the interfaces are neglected. This again shows that properly taking into account the interface layers is important.

V. ELECTROREFRACTION

We finally apply our model to electrorefraction by applying a Kramers–Kronig transform to the calculated electroabsorption spectra. We also add the Pockels effect in order to be able to compare with our measured electrorefraction data. In Fig. 5, the calculated room temperature absorption

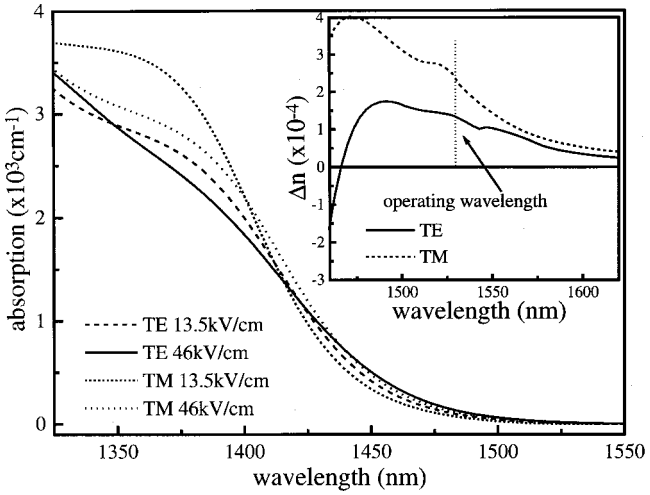

FIG. 5. Calculated room temperature absorption spectra for the CQW sample with 58.5% Ga for TE and TM polarization. The inset shows the electrorefraction calculated with these spectra.

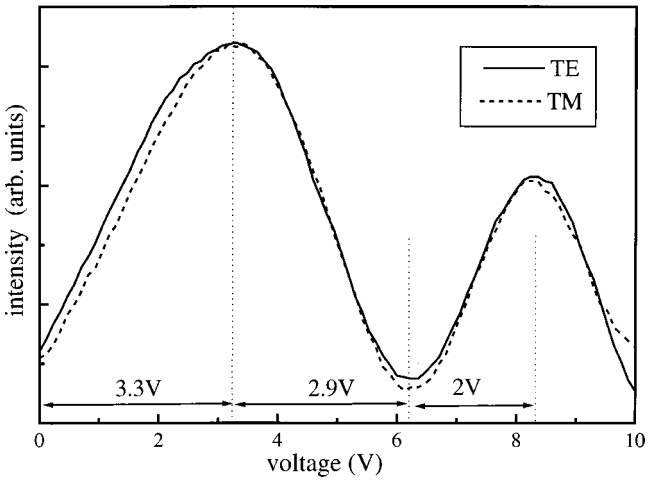

FIG. 6. Observation of polarization independent switching voltages for an MZI with −0.85% strained CQWs at 1525 nm.

spectra and electrorefraction spectra are shown for the CQW sample with 58.5% Ga, which is expected to be nearly polarization independent. The figure displays the absorption coefficient for the whole CQW film layer, thus including the 155 Å InP barriers. The spectra were convoluted with a 45 meV wide hyperbolic cosine, where the width was chosen equal to the width of the measured room temperature photoluminescence spectra. The exact spectral positions of the calculated absorption spectra were fixed by photocurrent measurements. Electrorefraction spectra, as shown in the inset of Fig. 5, were subsequently calculated by applying a Kramers–Kronig transform. We find an electrorefraction of 1.3×10^{-4} at 2.97 V and of 3.2×10^{-4} at 5.58 V applied bias for TE polarization. For TM polarization we calculate an electrorefraction of 2.35×10^{-4} at 2.97 V and 6.2×10^{-4} at 5.58 V applied bias. These values for the electrorefraction should be multiplied with an overlap factor of 0.42 between the waveguide mode and the quantum well material. Although the heavy hole is the uppermost valence band for this amount of strain, we observe that the calculated electrorefraction is larger for TM than for TE polarization for this sample.

In order to compare with experiment, the Pockels effect should also be taken into account. Electrorefraction due to the Pockels effect is positive for TE polarization in waveguides lined out along the $[1\bar{1}0]$ axis,[18,19] and is zero for TM polarization. We estimate the average electro-optic coefficient (r_{41}) in the intrinsic region to be -1.5×10^{-12} m/V,[19,20] resulting in a TE electrorefraction due to the Pockels effect of $\Delta n_{\mathrm{TE}}=2.4\times10^{-5}/\mathrm{V}$.[21] Taking the overlap between the waveguide mode and the active material to be 1.0 for the Pockels effect, we find a switching voltage of 3.98 V for TE and 4.52 V for TM polarization at 1530 nm. The CQW with 58.5% Ga thus shows nearly polarization independent electrorefraction with a switching voltage of 4.3 ± 0.3 V.

In order to measure the electrorefraction, the CQW material was processed into a Mach–Zehnder Interferometric switch (MZI) containing 4 mm long phase shifting sections. The measured switching curves are shown in Fig. 6. Although the waveguide losses were not equal for both polarizations, which required a vertical scaling of the two curves shown in Fig. 6, we observe a polarization independent switching voltage of 3.3 ± 0.05 V in the first switching point. Considering the complexity of the model, the measured switching voltage is quite close to the calculated switching voltage of 4.3 ± 0.3 V, showing that our model can be used as an accurate design tool for predicting device performance.

VI. SUMMARY

In summary, we presented a model for calculating the electrorefraction in strained InGaAs/InP quantum well structures using the 4×4 Luttinger–Kohn Hamiltonian. It was essential to take into account the strained InAs and InGaAsP interface layers around each InGaAs well in order arrive at the correct band gap and polarization dependence. We verified and tested the model on strained InGaAs/InP CQWs consisting of three 27 Å InGaAs quantum wells and two 15 Å barriers. These CQWs combine a QCSE redshift as large as 60 meV at 11.7 V bias with waveguide transparency at 1.55 μm. The observed redshift is two times larger than in a quaternary well of the same total thickness. When the interface layers were taken into account, our model is in excellent agreement with the measured electroabsorption spectra. When we inserted the CQW material in a MZI switch, we find a polarization independent switching voltage of 3.3 V at 1530 nm. The measured switching voltages were found to be quite close to the calculated switching voltages of 4.3 ± 0.3 V when the Pockels effect was also taken into account. We finally conclude that the model can serve as an accurate design tool for predicting device properties and for improving their performance.

ACKNOWLEDGMENTS

The authorS thank M. Kemerink for providing us with a computer code for solving the 4×4 Luttinger–Kohn Hamiltonian. They also thank D. H. P. Maat and F. H. Groen from the Applied Optics group of the Delft University of Technology for processing their material into an MZI switch. This research is funded by the IOP Electro-Optics of the Dutch Ministry of Economic Affairs and the ACTS program of the European Union.

[1] I. Bar-Joseph, C. Klingshirn, D. A. B. Miller, D. S. Chemla, U. Koren, and B. I. Miller, Appl. Phys. Lett. **50**, 1010 (1987).
[2] H. Temkin, D. Gershoni, and M. B. Panish, Appl. Phys. Lett. **50**, 1776 (1987).
[3] J. E. Zucker, K. L. Jones, T. H. Chiu, B. Tell, and K. Brown-Goebeler, J. Lightwave Technol. **10**, 1926 (1992).
[4] T. Aizawa, K. G. Ravikumar, S. Suzaki and T. Watanabe, IEEE J. Quantum Electron. **30**, 585 (1994).
[5] J. M. Luttinger and W. Kohn, Phys. Rev. **97**, 869 (1955).
[6] R. T. H. Rongen, A. J. C. van Rijswijk, M. R. Leys, C. M. van Es, and J. H. Wolter, Semicond. Sci. Technol. **12**, 974 (1997).
[7] T. Marchner, J. Brübach, C. A. Verschuren, M. R. Leys, and J. H. Wolter, J. Appl. Phys. **83**, 3630 (1998).
[8] C. G. v.d. Walle, Phys. Rev. B **39**, 1871 (1989).
[9] M. P. C. M. Krijn, Semicond. Sci. Technol. **6**, 27 (1991).
[10] O. Madelung and M. Schulz, *Landolt-Börnstein*, Vol. 22a (Springer, Berlin, Germany, 1987).
[11] R. Winkler, Phys. Rev. B **51**, 14395 (1995).

[12] J. S. Weiner, D. A. B. Miller, and D. S. Chemla, Appl. Phys. Lett. **50**, 842 (1987).
[13] D. A. B. Miller, J. S. Weiner, and D. S. Chemla, IEEE J. Quantum Electron. **QE-22**, 1816 (1986).
[14] C. G. M. Vreeburg, M. K. Smit, M. Bachman, R. Kyburz, R. Krähenbühl, E. Gini, and H. Melchior, Proceedings 7th European Conference on Integrated Optics (ECIO'95), Delft, the Netherlands, 1995, p. 225.
[15] J. E. Zucker, M. D. Divino, T. Y. Chuang, and N. J. Sauer, Electron. Lett. **30**, 518 (1994).
[16] N. Susa, J. Appl. Phys. **73**, 8463 (1993).
[17] M. Suguwara, T. Fujii, S. Yamazaki, and K. Nakajiama, Phys. Rev. B **42**, 9587 (1990).
[18] M. Glick, F. K. Reinhart, G. Weimann, and W. Schlapp, Appl. Phys. Lett. **48**, 989 (1986).
[19] S. Adachi and K. Oe, J. Appl. Phys. **56**, 74 (1984).
[20] J. E. Zucker, I. Bar-Joseph, B. I. Miller, U. Koren, and D. S. Chemla, Appl. Phys. Lett. **54**, 10 (1989).
[21] S. Adachi, *Physical Properties of III-V Semiconductor Compounds* (Wiley, New York, 1992); C. E. Soccolich, Appl. Phys. Lett. **49**, 1602 (1986).